Isomers and Transition States of the Na_4^+ Clusters. Ab Initio Studies of Geometries and Absorption Spectra

Kenji Mishima

Department of Applied Chemistry, Graduate School of Engineering, The University of Tokyo, Tokyo, Japan 113

Koichi Yamashita*

Department of Chemical System Engineering, Graduate School of Engineering, The University of Tokyo, Tokyo, Japan 113

André Bandrauk

Laboratoire de Chimie Théorique, Faculté des Sciences, Université de Sherbrooke, Sherbrooke, Québec, J1K 2R1, Canada

Received: October 31, 1997; In Final Form: February 20, 1998

Stable isomers, transition states, and their photoabsorption spectra for the Na_4^+ cluster are determined by ab initio MRCI calculations. Three stable geometries of symmetry C_{2v}, D_{2h}, and D_{2d} and two transition states of symmetry C_s and C_2 are identified. The D_{2d} configuration is a new geometry not previously obtained in ab initio calculations. The photoabsorption spectra of the three isomers and the transition states are used to interpret experimental absorption data. Dissociation dynamics and possible laser control of isomer populations are discussed in terms of the electronic states of the cluster.

Introduction

Alkali metal clusters offer model systems for studying the transition from atomic to molecular to condensed matter due to the relatively small number of their valence electrons. Theoretical descriptions range from the free electron jellium model of charge clusters[1] to the molecular description more appropriate for small clusters.[2] Na clusters have been recently examined in detail experimentally[3−5] and by ab initio quantum chemical calculations.[6,7] Temperature measurements in small Na cluster ions, Na_n^+ ($n = 4, 7, 11$), exhibit unexpectedly large temperature dependence of absorption spectra. In particular, it was found that small cold clusters are best described by ab initio quantum chemical calculations.[3−8] Further experimental work on dissociation dynamics of these small ion clusters ($n \leq 11$) points to the applicability of orbital correlation diagrams,[8] thus further underpinning the usefulness of a molecular description. As emphasized previously by Haberland,[9] ion clusters exhibit stronger bonding than neutrals and optical absorption spectra always shift to the visible, thus rendering ion clusters more accessible experimentally. The charge seems to be localized in rare gas clusters but not in metals. From a theoretical viewpoint, the hole created by removing one electron increases the number of optically allowed transitions with strong transition moments of the large resonance type,[10] and geometrical structures due to electron orbital degeneracies are Jahn−Teller unstable as calculated before in H_n^+ species.[11−13] The strong transition moments and low ionization potentials suggest metal clusters as excellent candidates for high-order harmonic generation in strong laser fields.[14] In the present work, we concentrate on calculating stable geometries, isomerization paths, and absorption spectra of the cluster using ab initio MRCI methods in order to explore the possibility of optically preparing various isomers by pump−dump laser schemes which are equivalently Raman-stimulated processes. In particular, our previous work on chirped pulse Raman adiabatic passage[15,16] suggested some efficient methods of inverting and transferring populations in symmetric systems in analogy to chirped pulse IR laser excitation.[16−18] The present ab initio results are used to assess the feasibility of laser methods to control molecular populations in clusters.

Method of Calculation

For the geometry optimization, the level MP2 was adopted with the 6-31G* basis set. To determine whether the optimized geometries are stable or not, we calculated their harmonic frequencies. After obtaining the stable and transition state geometries, we calculated more accurate ground and excited-state energies and transition dipole moments between the ground and some excited states. The multireference configuration−interaction (MRCI) approach is used in order to include the electron correlation effects. As a basis set, we used the effective core potential (ECP) for the inner shell and the basis function (4s4p/2s2p) for the valence orbitals, which was determined for the ECP. We added the d function with exponent 0.09 to this ECP.[7]

To calculate transition dipole moments, state averaging was done: five $^2A_1$, three $^2B_1$, five $^2B_2$, and two $^2A_2$ (MRCI level) and nine $^2A_1$, six $^2B_1$, eight $^2B_2$, and three $^2A_2$ (CASSCF level) for C_{2v}. For the geometries of D_{2h}, D_{2d}, C_s, and C_2, the same level of state averaging was adopted. Details concerning each of these isomers are mentioned in the next section. We employed GAUSSIAN94[19] for geometry optimizations and harmonic frequency calculations and MOLPRO96[20] for calculating excitation energies and transition dipole moments.

S1089-5639(98)00036-X CCC: $15.00
Published on Web 04/14/1998

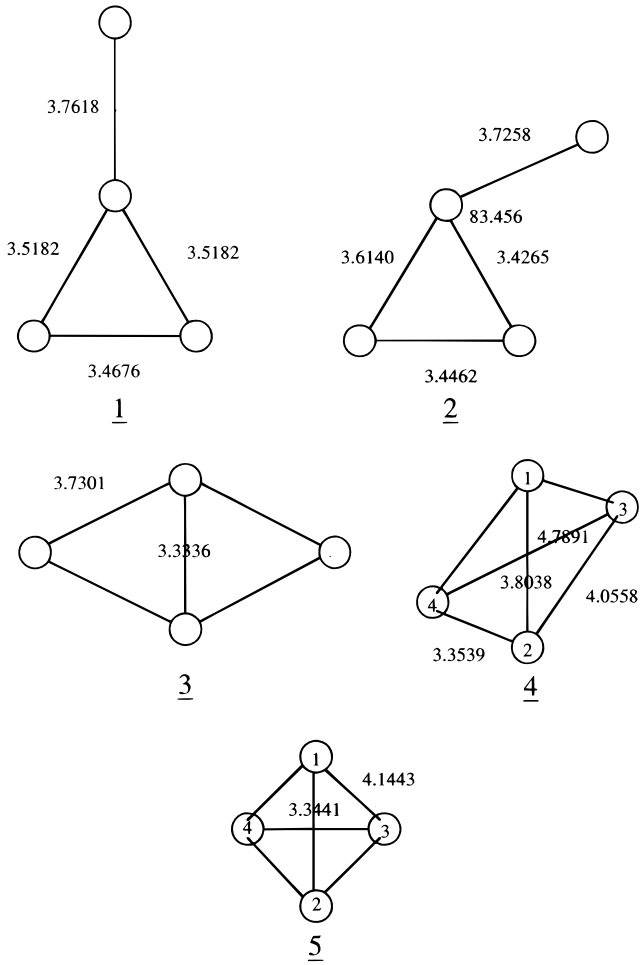

Figure 1. Optimized geometries of the Na_4^+ cluster with bond lengths in angstroms and angles in degrees. The point groups are **1** (C_{2v}), **2** (C_s,) **3** (D_{2h}), **4** (C_2), and **5** (D_{2d}). The geometries **1**, **3**, and **5** are stable states while **2** and **4** are transition states. The distances between the bonds 1−2 and 3−4 are 2.1209 (**4**) and 3.4035 Å (**5**), respectively.

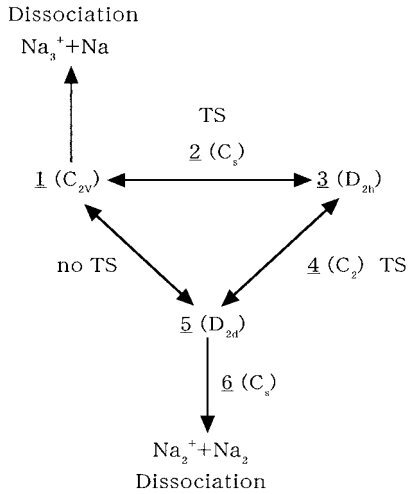

Figure 2. Isomerization path of the Na_4^+ cluster. For details, see the text.

Results

The MP2/6-31G*-optimized geometries are shown in Figure 1 and the isomerization path of Na_4^+ cluster is shown in Figure 2. As Table 1 shows, our CASSCF and MRCI calculations predict similar relative stability among the stationary geometries. Stable **1** (C_{2v}) and **3** (D_{2h}) geometries are the same as those obtained by Bonačić-Koutecký et al.[7] Their ground states belong to 1^2A_g and 1^2B_{3u}, respectively. As compared with the full CI results by Bonačić-Koutecký et al.,[7] the bond lengths are generally longer. As they pointed out, the bond lengths calculated by the SCF method are longer than those obtained by the full CI method in the case of alkali metal clusters. This is because alkali metal clusters are inclined to delocalize their electrons according to the multicentered structures. The neglect of this effect when geometry is optimized may lead to deviations from the experimentally observed results or spectra. As MP2 takes into account electron correlations, our bond length results are suitable for the energetics calculation.

The stable geometry **5** (D_{2d}) is a new configuration. Such tetrahedral structures have been predicted in Li_4^{2+} and Na_4^{2+} to be stabilized by p orbitals.[21] Although the ground states of **1** (C_{2v}) and **3** (D_{2h}) are almost degenerate as shown in Table 1 (*1* (C_{2v}) is higher in energy by 0.017 eV than **3** (D_{2h}) at the MRCI level), **5** (D_{2d}) is slightly higher than **1** (C_{2v}) and **3** (D_{2h}) (by 0.081 eV with respect to **3** (D_{2h}) at the MRCI level). Nevertheless, as expected from their relatively long bond lengths, the three stable states are almost degenerate, which prevents us from determining correctly the order of energy levels of the various geometries. The energy differences are sensitive to the method and basis functions. At the CASSCF and MRCI levels, **3** (D_{2h}) is the most stable geometry. It is also so in the calculation of Bonačić-Koutecký et al.,[7,22] using the full CI and basis set (ECP with basis set (4s3p1d/3s3p1d)).

As transition states, two geometries **2** (C_s) and **4** (C_2) were found (Figure 1). Geometry **2** connects the reaction path between the ground states of **1** (C_{2v}) and **3** (D_{2h}). The relatively long external bond length (3.7618 Å) of **2** (C_s) makes the energy barrier between the stable states of **1** (C_{2v}) and **3** (D_{2h}) quite shallow (cf. Table 1). Therefore, the geometry transformation between **1** (C_{2v}) and **3** (D_{2h}) takes place easily. There is a similar example, the H_4^+ cluster. For the H_4^+ cluster with C_{2v} geometry, which is analogous to geometry **1**, the hydrogen atom that is located at the apex of the planar triangle H_3^+ is quite mobile in the plane defined by the three hydrogen atoms of the planar triangle. It is reported that the bond length between the hydrogen atom and the adjacent atom is 1.850 Å while the other bond lengths are 0.876, 0.905, and 0.905 Å.[13] We attempted intrinsic reaction coordinate (IRC) calculations between **1** (C_{2v}) and **3** (D_{2h}) through **2** (C_s). The calculated imaginary frequency (30.3 i cm^{-1}) of **2** (C_s) was too small to obtain the IRC numerically.

The transition state **4** (C_2) connects **3** (D_{2h}) and **5** (D_{2d}). Originally, we obtained a geometry of C_1 symmetry instead of C_2 for **4** (C_2). In the C_1 geometry, two bonds with length 4.0558 Å in **4** are replaced by 4.0556 and 4.0560 Å. Both geometries are the transition states with an imaginary frequency of 36.1 i cm^{-1} by harmonic frequency analysis. The energy of the C_1 symmetry was found to be −0.641 003 au which is equal to that of **4** (C_2) (cf. Table 1). Because there is no energy difference and almost the same geometry between C_1 and **4** (C_2), we adopt **4** (C_2) as a transition state. A candidate for the simplest reaction path is through folding of the **3** (D_{2h}) along the shorter diagonal line, retaining C_{2v} symmetry and leading to **5** (D_{2d}). However, we failed to calculate IRC because the imaginary frequency 36.1 i cm^{-1} is too small to solve the IRC equation numerically.

We tried to find a transition state between **1** (C_{2v}) and **5** (D_{2d}), but in vain. This would give some hint as to why only the absorption spectral peaks of **3** (D_{2h}) are observed in the experimental spectra. In the unlooped geometry transformation

TABLE 1: Ground-State Energies and Energy Differences from C_{2v} Geometry[a]

geometry	state	HF (au)	ΔE_{HF} (eV)	CASSCF (au)	ΔE_{CASSCF}	MRCI (au)	ΔE_{MRCI} (eV)
C_{2v}	$^2A_1$	−0.612 076	0.0	−0.642 920	0.0	−0.643 276	0.0
D_{2h}	$^2B_{3u}$	−0.637 490	0.692	−0.643 354	−0.012	−0.643 908	−0.017
D_{2d}	$^2A_1$	−0.599 379	0.348	−0.640 105	0.077	−0.640 946	0.063
C_s	$^2A'$	−0.607 806	0.116	−0.642 297	0.017	−0.642 748	0.014
C_2	^2A	−0.599 633	0. 339	−0.640 341	0.070	−0.641 003	0.062

[a] The data were calculated by using the ECP for the inner shell and the basis function (4s4p/2s2p) for the valence orbitals determined for the ECP. The sign Δ is used to represent the energy difference from C_{2v} geometry.

1 (C_{2v}) **2** (C_s) **3** (D_{2h}) **4** (C_2) **5** (D_{2d}), **3** (D_{2h}) is visited twice in contrast with **1** (C_{2v}) and **5** (D_{2d}), which are visited only once. If the geometry transformation were looped, the three stable geometries would appear in the spectra equally.

In Figure 3, we demonstrate the absorption spectra calculated for the three stable (**1** (C_{2v}), **3** (D_{2h}), **5** (D_{2d})) and two transition-state (**2** (C_s), **4** (C_2)) geometries, respectively. In Figure 4, we show the recent absorption spectra obtained experimentally by Ellert et al.[5] Among low-lying excited states of Na_4^+, some states have zero transition dipole moments due to selection rules. We calculated as many states as possible including these "dark" states because we are interested in how the energy levels of the ground and excited states and transition dipole moments change along the isomerization reaction path. For both of the transition states **2** (C_s) and **4** (C_2), we managed to include up to 10 states in the MRCI calculation (not shown). It should be pointed out that CASSCF and MRCI transition dipole moments are generally in good agreement for Na_4^+ clusters.

For both **1** (C_{2v}) and **2** (C_s), Bonačić-Koutecký et al.[7] have calculated three prominent peaks which coincide more or less with the experimental spectra obtained by Ellert et al.[3] But a one-to-one correspondence of the peaks has not yet been achieved. Comparing our results with the experimental ones and those of Bonačić-Koutecký et al.,[7] we found some peaks red-shift and others blue-shift in our results. The three prominent experimental peaks are located at 1.95, 2.76, and 3.22 eV.[7] The peaks of 3^2A_1, 3^2B_2, and 3^2B_1 states of **1** (C_{2v}) are located at 1.92, 2.58, and 3.06 eV in our MRCI results, while they are at 2.04, 2.74, and 3.26 eV in Bonačić-Koutecký et al.[7] The peaks of 2^2A_g, 2^2B_{1g}, and 2^2B_{2g} states of **2** (C_s) are located at 1.83, 2.65, and 3.08 eV in our MRCI results, while they are at 1.93, 2.80, and 3.30 eV in Bonačić-Koutecký et al.[7]

On the other hand, the calculated spectrum of the new D_{2d} symmetry **5** (D_{2d}) has quite different features (Figure 3 e,h). In **1**, $^2B_1$ and $^2B_2$ states are degenerate. There is a strong peak around 2.6 eV, a smaller peak at 2.04 eV, and much smaller ones at 3.05 and 3.26 eV. The strong peak comprises three excited states: 5^2A_1, 3^2B_1, and 3^2B_2. This strongest peak at 2.6 eV coincides with the peaks obtained for **1** (C_{2v}) and **3** (D_{2h}) while the other peaks do not appear in the experimentally obtained photodepletion spectrum. This drastic difference may be caused by a significant change in the molecular structure. As already mentioned above, **5** (D_{2d}) has a relatively higher energy (0.06 eV). Therefore, at the low temperature, 35 K, at which the experiment was conducted, almost all the molecules probably exist in the lowest **1** (C_{2v}) and **3** (D_{2h}) geometries while the population of **5** (D_{2d}) could be small. Ellert et al.[3] reproduced the experimental photodepletion spectrum of Na_4^+ at 700 K. The spectrum shows a strong temperature dependence. There are three prominent peaks with a broad spectral width which red-shift significantly as the temperature rises. Our results suggest that the spectral line broadening is brought about by not only the temperature but also the increase in the population of **5** (D_{2d}).

The absorption spectrum of **2** (C_s) resembles spectra of **1** (C_{2v}) and **3** (D_{2h}). In particular, all three are similar in that they have three strong peaks around the same energy. Referring to character tables, we see the A_1 and B_2 states of C_{2v} geometry correlate to the A′ state of C_s geometry and A_2 and B_1 states, to the A″ state of C_s geometry. In the same way, the A_g and B_{1g} states of D_{2h} geometry correspond to A′ states of C_s geometry and B_{2g}, to A″ of C_s geometry. By checking the energy sequence of **1** (C_{2v}) and **3** (D_{2h}) in the C_s group, taking into account the nonadiabatic curve crossings, it can be confirmed that, in the isomerization from **1** (C_{2v}) to **3** (D_{2h}), 3^2A_1, 3^2B_2, and 3^2B_1 states of **1** (C_{2v}) are connected with 2^2A_g, 2^2B_{1g}, and 2^2B_{2g} states of **3** (D_{2h}), respectively. At the MRCI level, the peaks of the states $5^2A'$, $8^2A'$, and $4^2A''$ are situated at 1.85, none, and 3.16 eV, respectively. These values are in a good agreement with those of **1** (C_{2v}) and **3** (D_{2h}) at each calculation level. In summary, in the reaction path from **1** (C_{2v}) to **3** (D_{2h}) retaining C_s symmetry, no remarkable change is observed in the transition dipole moments.

As for **4** (C_2), at the CASSCF level, many small peaks are found at the higher energy range. Therefore, we analyzed the excited states of **5** (D_{2d}) using the CASSCF data. The spectrum of **4** (C_2) resembles that of **5** (D_{2d}) rather than **3** (D_{2h}). The main peak in the range from 2.6 to 3.0 eV consists of three states. The difference is that there are two peaks below the main peak for **4** (C_2) and the three broad peaks above the main peak consist of four peaks for **3** (D_{2h}) contrary to many small peaks for **4** (C_2).

In comparison with the reaction path from **1** (C_{2v}) to **3** (D_{2h}) via **2** (C_s), drastic changes in the oscillator strengths were observed. A_g, B_{1g}, B_{1u}, and A_u states of **3** (D_{2h}) are correlated with the A state of **4** (C_2) while B_{3u}, B_{2u}, B_{2g}, and B_{3g} are with the B state. In the same way, the A_1 and A_2 states of **5** (D_{2d}) are connected with the A state of **4** (C_2) while B_1 and B_2 states are with the B state. By looking into the energy sequence of **3** (D_{2h}) and **5** (D_{2d}) in the C_2 symmetry, we determined the change of the oscillator strengths from **3** (D_{2h}) and **5** (D_{2d}) through **4** (C_2). The state 2^2A_g of **3** (D_{2h}) corresponds to the 4^2A state of **4** (C_2), which links with 3^2A_1 state of **5** (D_{2d}) whose oscillator strength is relatively small. In this case, the oscillator strength decreases monotonically. The state change from 2^2B_{2g} through 8^2B to 4^2B_1 or 4^2B_2 also belongs to this type. The state 2^2B_{1g} of **3** (D_{2h}) corresponds to 7^2A state of **4** (C_2), which links with 5^2A_1 state of **5** (D_{2d}). In this case, the oscillator strengths of the stable geometries and those of the transition state show no remarkable difference.

Discussion

The photodepletion spectra of Na_4^+ and previously published data at low temperatures[3,4] agree remarkably well with our calculated optically allowed transitions for the **3** (D_{2h}) geometry. Thus, the three strong peaks at 1.95, 2.76, and 3.22 eV observed experimentally agree quite well with all four geometries, **1** (C_{2v}), **2** (C_s), **3** (D_{2h}), and **4** (C_2). In view of the low barriers *E* (Table

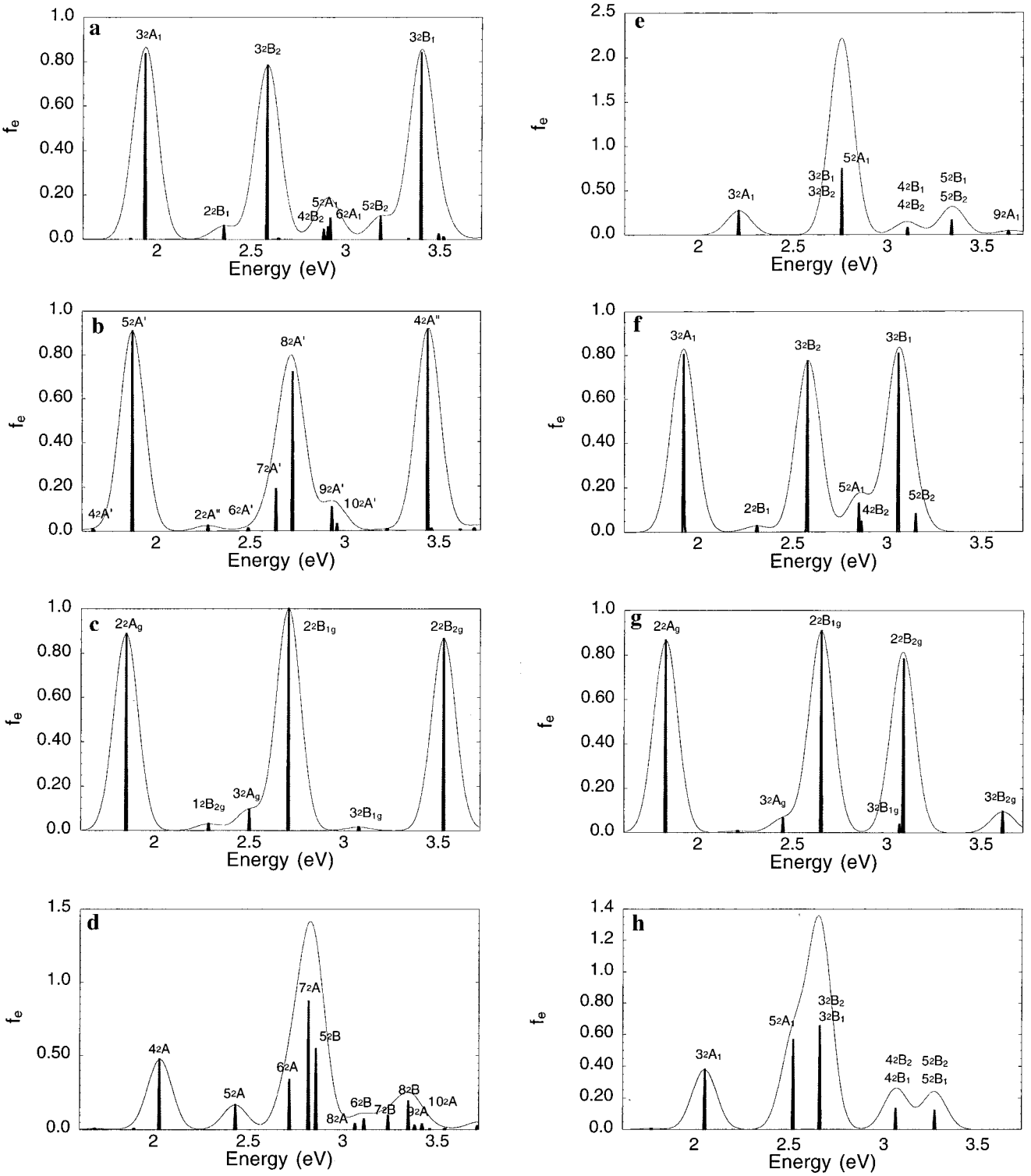

Figure 3. Absorption spectra of the Na_4^+ cluster obtained by ab initio calculations. The abscissa represents excitation energy from the ground state and the ordinate, oscillator strength. The bold lines in the figure are the oscillator strengths for each excited state. The smooth curves around the peaks are superpositions of Gaussian lines. The spectra are for (a) C_{2v}, (b) C_s, (c) D_{2h}, (d) C_2, and (e) D_{2d} by CASSCF and (f) C_{2v}, (g) D_{2h}, and (h) D_{2d} by MRCI.

1) between the **1** (C_{2v}) and **3** (D_{2h}) structures, 115 cm^{-1} from **1** (C_{2v}) to **2** (C_s) and 253 cm^{-1} from **3** (D_{2h}) to **2** (C_s), the shifting of the high-energy absorption peaks (2.8 and 3.3 eV) to lower energies with increasing temperature[7] is consistent with the increasing contribution of the **2** (C_s) transition state to the absorption spectrum. The shifting of the lowest energy peak (1.9 eV) to higher energies with increasing temperature[7] indicates some contribution of the **2** (C_s) transition state and **5** (D_{2d}) isomer, the new geometry obtained in our calculations. Our calculated **3** (D_{2h}) spectrum further shows a fourth peak at 3.7 eV, in agreement with the experimental data.[4] A very weak, but sharp peak, observed experimentally at 2.32 eV at very low temperatures (35 K), that is identical to the Na_2^+ transition,[4,5] also appears as a side peak in the **1** (C_{2v}), **2** (C_s), and **3** (D_{2h}) geometries but is absent in the **4** (C_2) and **5** (D_{2d}) geometries. This is in agreement with the low population of **4** (C_2) and **5** (D_{2d}) geometries due to their higher energies (630−650 cm^{-1}) above the ground **3** (D_{2h}) isomer. Thus, at low temperatures

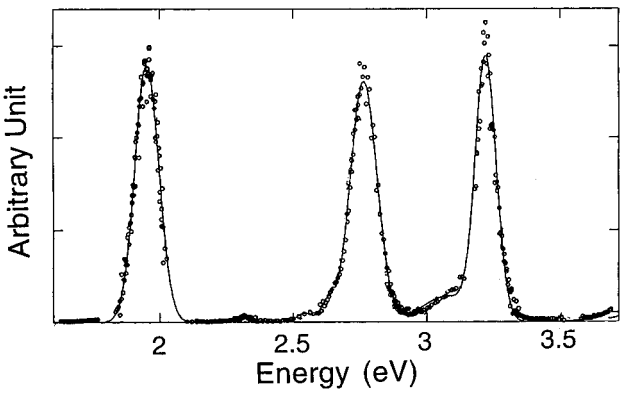

Figure 4. Experimental absorption spectra of the Na_4^+ cluster. The dots are the experimentally observed absolute photoabsorption cross sections. The bold smooth lines in the figure are superpositions of Gaussian lines.

(T < 100 K), the relevant structures are **1** (C_{2v}), **2** (C_s), and **3** (D_{2h}) with the **2** (C_s) transition state visited twice during the isomerization process between the first (*1* (C_{2v})) and third (*3* (D_{2h})) structures (Figure 1).

Recent collision-induced dissociation experiments by Nonose et al. on Na_n^+ clusters[8] have shown the propensity for even-numbered cluster ions Na_{2n}^+ to release Na atoms, predominantly at low rare gas atom impact energies, and with increasing Na_2 release at higher impact energies. Thus, in the case of Na_4^+ these results imply that the atomic channel

$$Na_4^+ \rightarrow Na_3^+ + Na \qquad (1)$$

has a lower dissociation energy than the molecular channel

$$Na_4^+ \rightarrow Na_2^+ + Na_2 \qquad (2)$$

In fact, from the ab initio calculations we arrive at the conclusion that dissociation products in reaction **2** are 0.50 eV (at the MRCI level) above the dissociation limit of channel 1. This is due to the unusual high stability of the Na_3^+ ion. A similar result is found for the H_4^+ ion;[11] i.e., the reaction path from $H_2^+ + H_2$ to $H_3^+ + H$ is essentially "downhill". Thus, clearly after collision with an external atom, the **3** (D_{2h}) isomer is easily excited to the **1** (C_{2v}) geometry, which then easily dissociates to $Na_3^+ + Na$. We have found no transition state from **1** (C_{2v}) to **5** (D_{2d}) as discussed in the previous section. At high collision energies, the **5** (D_{2d}) isomer can be expected to become populated. A stationary point **6** (C_s) with one imaginary frequency 113.8 i cm^{-1} at the MP2 level was found for the reaction path from **5** (D_{2d}) to $Na_2^+ + Na_2$. However, the isomers **5** (D_{2d}), **6** (C_s), and $Na_2^+ + Na_2$ have the energies −647.2621, −647.2570, and −647.2345 au at the MP2 level and −0.6409, −0.6359, and −0.6080 au at the MRCI level, respectively. Therefore, we may conclude that the reaction path from **5** (D_{2d}) to $Na_2^+ + Na_2$ is merely repulsive. Our minimum energy path showed a path having a C_s geometry, consistent with a short-bond Na_2 and long-bond Na_2^+ dissociation channel. Thus, to conclude our photodissociation dynamics discussion, the predominance of channel 1 is consistent with the low energy of the **1** (C_{2v}) isomer and the high stability of the odd-numbered cluster, Na_3^+. It is to be noted that experimentally larger odd-numbered cluster ions Na_{2n+1}^+ always dissociate to lower odd-numbered ions Na_{2n-1}^+ and Na_2[8] is therefore also a consequence of the high stability of odd-numbered cluster ions.

The low barrier (see Table 1) between the most stable isomers, **1** (C_{2v}) and **3** (D_{2h}), implies that we must go to very low temperatures (T < 75 K for $\Delta E \sim 250$ cm^{-1}) in order to isolate the lowest energy **3** (D_{2h}) isomer. At such low temperatures, the photoabsorption spectra of Figure 3 show the strong transitions which maintain their oscillator strengths along the isomerization path. This would make feasible studies of optical interconversion between these two isomers by a resonant or nonresonant chirped Raman scheme[15,16] in order to elucidate the isomerization dynamics.

The **3** (D_{2h}) to **5** (D_{2d}) optically induced isomerization along the ground-state isomerization path would be much less efficient due to the much weaker absorption spectra of the **4** (C_2) transition state. A further investigation of the excited states is required to discover the optimal optical isomerization path in this latter case. Recent theoretical improvements on calculations of vibrational structures of weakly bound tetraatomic systems[24] will be useful for investigating further the isomerization dynamics of optically prepared higher energy isomers in the ion cluster and others discussed in the present paper.

Acknowledgment. We thank Dr. Ch. Ellert for discussions of his experimental results and Prof. V. Bonačić-Koutecký for theoretical discussions. The present work is partially supported by a Grant-in-Aid for Scientific Research from the Japanese Ministry of Education, Science, and Culture.

References and Notes

(1) Brack, M. *Rev. Mod. Phys.* **1993**, *65*, 677.
(2) *Clusters of Atoms and Molecules*; Haberland, H., Ed.; Springer Series in Chemical Physics 52; Springer: New York, 1994.
(3) Ellert, C.; Schmidt, M.; Schmitt, C.; Reiners, T.; Haberland, H. *Phys. Rev. Lett.* **1995**, *75*, 1731.
(4) Ellert, C. Ph.D. thesis, Universitat Freiburg, Germany, 1996.
(5) Ellert, C.; Schmidt, M.; Reiners, T.; Haberland, H. *Z. Phys. D* **1997**, *39*, 317.
(6) Bonacic-Koutecky, V.; Fantucci, P.; Koutecky, J. *J. Chem. Phys.* **1990**, *93*, 3802.
(7) Bonacic-Koutecky, V.; Pittner, J.; Fuchs, C.; Fantucci, P.; Guest, M. F.; Koutecky, J. *J. Chem. Phys.* **1996**, *104*, 1427.
(8) Nonose, S.; Tanaka, H.; Mizuno, T.; Kim, N. J.; Someda, K.; Kondow, T. *J. Chem. Phys.* **1996**, *105*, 9167.
(9) Haberland, H.; Issendorff, B. v.; Kolar, T.; Kornmeier, H.; Ludewigt, C.; Risch, A. *Phys. Rev. Lett.* **1991**, *67*, 3290.
(10) Bandrauk, A. D. *Molecules in Laser Fields*; (M. Dekker: New York, 1993; Chapters 1 and 3.
(11) Stine, J. R.; Muckerman, J. T. *J. Chem. Phys.* **1978**, *68*, 185.
(12) Wright, J. S.; DiLabio, G. A. *J. Phys. Chem.* **1992**, *96*, 10793.
(13) Jungwirth, P.; Cársky, P.; Belly, T. *Chem. Phys. Lett.* **1992**, *195*, 371.
(14) Zuo, T.; Bandrauk, A. D. *Phys. Rev. A* **1995**, *52*, R2511; **1996**, *54*, 3254.
(15) Chelkowski, S.; G. N. Gibson, *Phys. Rev. A* **1995**, *52*, R3417.
(16) Chelkowski, S.; Bandrauk, A. D. *J. Raman. Spectrosc.* **1997**, *28*, 459.
(17) Chelkowski, S.; Bandrauk, A. D.; Corkum, P. B. *Phys. Rev. Lett.* **1996**, *76*, 1445.
(18) Chelkowski, S.; Bandrauk, A. D. *Chem. Phys. Lett.* **1991**, *186*, 264.
(19) *GAUSSIAN 94* (Revision D. 1), Frisch, M. J.; Trucks, G. W.; Schlegel, H. B.; Gill, P. W. M.; Johnson, B. G.; Robb, M. A.; Cheeseman, J. R.; Keith, T. A.; Petersson, G. A.; Montgomery, J. A.; Raghavachari, K.; Al-Laham, M. A.; Zakrzewski, V. G.; Ortiz, J. V.; Foresman, J. B.; Cioslowski, J.; Stefanov, B. B.; Nanayakkara, A.; Challacombe, M.; Peng, C. Y.; Ayala, P. Y.; Chen, W.; Wong, M. W.; Andres, J. L.; Replogle, E. S.; Gomperts, R.; Martin, R. L.; Fox, D. J.; Binkley, J. S.; Defrees, D. J.; Baker, J.; Stewart, J. P.; Head-Gordon, M.; Pople, J. A. Gaussian, Inc., Pittsburgh, PA, 1995.
(20) MOLPRO is a package of ab initio programs written by H. J. Werner and P. J. Knowles, with contributions from J. Almlof, R. D. Amos, M. J. O. Deegan, S. T. Elbert, C. Hampel, W. Meyer, K. Peterson, R. Pitzer, A. J. Stone, and P. R. Taylor.
(21) Glukhovtsev, M. N.; von R. Schleyer, P.; Stein, A. *J. Chem. Phys.* **1993**, *97*, 5541.
(22) Bonacic-Koutecky, V.; Fantucci, P; Koutecky, J. *Chem. Rev.* **1991**, *91*, 1035.
(23) Huber, K. P.; Herzberg, G. *Spectroscopic Constants of Diatomic Molecules*; Van Nostrand: Princeton, NJ, 1979.
(24) Alvarez-Collado, J. R.; Aguado, A.; Paniagua, N. *J. Chem. Phys.* **1995**, *102*, 5725.